Hindawi
International Journal of Antennas and Propagation
Volume 2022, Article ID 4765008, 7 pages
https://doi.org/10.1155/2022/4765008

*Research Article*

# A Low-Profile Dual-Band Directional Antenna for Unmanned Aerial Vehicle Applications

**Hui Jin,[1] Chong-Zhi Han,[2] Yanzhi Fu,[3] and Huaiwen Yang[1]**

[1]*School of Electronics and Information Engineering, School of Integrated Circuit Science and Engineering, Beihang University, Beijing 100191, China*
[2]*School of Ocean Information Engineering, Jimei University, Xiamen 361021, China*
[3]*Shenzhen Academy of Metrology and Quality Inspection, Shenzhen 518073, China*

Correspondence should be addressed to Chong-Zhi Han; chongzhi_han@foxmail.com

Received 6 September 2022; Revised 22 September 2022; Accepted 5 October 2022; Published 17 October 2022

Academic Editor: Giovanni Andrea Casula



A low-profile dual-band directional antenna operating at both 2.4 and 5 GHz for wireless local area networks (WLANs) for unmanned aerial vehicles (UAVs) applications is proposed in the paper. Two pairs of dipole antenna arrays with different electrical lengths are utilized to achieve dual-band directional radiation performance, which is desirable for a remote-control unit of the UAVs. Note that the directional radiation characteristic is obtained according to the double-dipole antennas driven by antiphase signals (W8JK), provided the distances between different dipole antennas are properly optimized. Note that the distance between the two longer dipoles, as well as the two shorter dipoles, can be calculated by equations. For each pair of dipoles with equal electrical lengths, an antiphase along the two dipoles can be obtained, and directional radiation characteristics can be achieved in the dual band. Coplanar strips (CPS) are employed as feeding networks, which lie on the same substrate layer as the antenna arrays, resulting in a low profile of merely 0.762 mm. Also, the overall size of the antenna together with the feeding network is $58.42 \times 32.58 \times 0.762\ \text{mm}^3$. To verify the performance of the proposed antenna, a prototype is fabricated and measured. The measured gain is 5.2 and 7.0 dBi, respectively, in the 2.4 and 5.8 GHz bands. The measured reflection coefficients as well as radiation patterns are consistent with those of the simulated results. The proposed antenna scheme can be a good candidate for UAV applications with the advantages of a lower profile, dual-band characteristics, directional radiation characteristics, and a simple assembly. Since the remote-control unit operates at 2.4 GHz and 5.8 GHz to control the UAV unit, the low-profile dual-band directional radiation antenna has extensive application prospects when integrated into the space-limited unit.

## 1. Introduction

Unmanned aerial vehicles (UAVs) are desirable for further miniaturization. This is challenging since multiple communication systems such as navigation, image transmission, and remote-control are urgently are in need of integration [1]. Accordingly, low-profile and multiband antennas are attractive for UAV applications. And wireless local area networks (WLANs) are generally used for the remote-control system. Considering the scenario shown in Figure 1, in which the remote-control unit cooperatively operates with the UAVs, directional radiation antennas covering the WLANs bands are suitable choices. Moreover, as illustrated in Figure 1, lower backward radiation of the antenna integrated into the remote-control unit is required to mitigate the electromagnetic interference from nearby electronic devices. Meanwhile, forward radiation needs to be enhanced to ensure communication quality with the UAVs units. Because the UAVs always work overhead of the remote-control unit, in which the directional radiation characteristic is required. Moreover, the 2.4 GHz, as well as the 5.8 GHz, are normally utilized to operate cooperatively between the remote-control unit and the UAVs. Hence, a dual-band directional radiation antenna scheme might be a good candidate in the scenario shown in Figure 1.

To achieve directional radiation, several techniques have been reported [2–18]. The end-fire directivity of a linear periodic array with $N$ isotropic radiators can reach $N^2$ by

Table 1: Funding statement.

| Name of the funding | Funding number |
|---|---|
| Natural Science Foundation of Fujian Province | 2021J05178 |
| Scientific Research Foundation of Jimei University | ZQ2021001 |
| Natural Science Foundation of China | 12104027 |

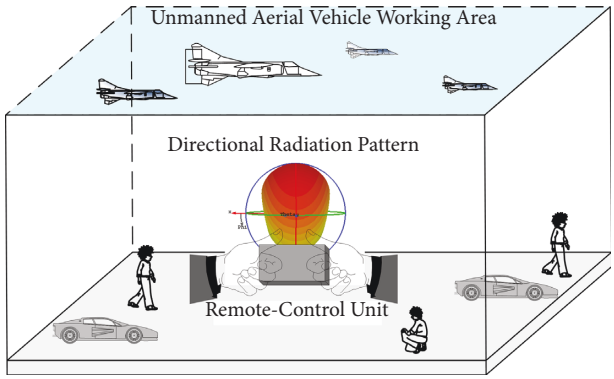


Figure 1: Directional radiation pattern of the remote-control unit for UAV applications.

decreasing spacing between elements, provided that the magnitudes and phases of the input excitations are properly chosen [2, 4]. Hence, in principle, the directional radiation characteristic can be obtained by two or more antenna elements at a certain frequency. A pair of double-dipole antennas driven by antiphase signals (W8JK) are typical representatives of the abovementioned linear periodic directional arrays, which are realized with two dipole antennas fed by antiphase signals [5, 6]. However, the design of a dual-band dipole linear periodic array/W8JK array becomes extremely complicated even for a 4-element array. On the one hand, the mutual couplings between elements are more difficult to minimize. On the other hand, the antiphase feeding network with desired excitation magnitudes of a dual-band linear periodic/W8JK array will be more complicated. Similar to linear periodic antenna arrays, the $2 \times 3$ antenna array proposed in [7] can also achieve directional radiation characteristics with high gain. Another technique adopted for high directivity involves an additional ground plane as a reflector [8, 9], resulting in a high profile. For instance, the dimension of the dual-band high-gain antenna for 2.4 and 5 GHz wireless applications in [8] is $100 \times 60 \times 12\ \text{mm}^3$. Although the gain is satisfactory, the high profile limits its practical implementation for UAVs. Moreover, a dual-band directional slot antenna for Wi-Fi applications was introduced in [10] with a size of $90 \times 80 \times 36.5\ \text{mm}^3$. Front-to-back ratio (F/B ratio) up to 16 dB can be achieved at the expense of a high profile (36.5 mm).

Furthermore, it is expected that the beams in both the lower and upper bands are nonsplitting, and the horizontal beamwidths are approximately the same in certain scenarios [10]. Hence, similar beamwidths are always needed for dual-band antenna applications. While the electrical size would be much bigger in the upper bands, and the beamwidths of the main lobe would rapidly decrease for the upper bands. The antenna proposed in [10] partially conquers the issue, and the beamwidth shift is decreased to 21–30%.

In this letter, a low-profile dual-band directional antenna is introduced for UVAs applications. Compared with recent relevant works, the proposed antenna is superior in its extremely low profile. The dual-band directional antenna has a low profile of 0.762 mm with acceptable realized gains of 5.2 and 7.0 dBi, respectively, in the 2.4 and 5.8 GHz bands. Moreover, the overall size of the antenna together with the feeding network is $58.42 \times 32.58 \times 0.762\ \text{mm}^3$, which is much smaller than those antennas in [1, 2, 4]. Moreover, similar beamwidths in the dual bands are achieved with smaller beamwidth shifts compared with antennas in [10, 11]. These characteristics make the proposed antenna extremely suitable for UAV applications.

## 2. Antenna Design and Analysis

The configuration of the proposed low-profile dual-band directional antenna is depicted in Figure 2, which consists of four dipole antennas and coplanar strips (CPS) as the feeding network. In Figure 2, longer yellow strips depict the dipole antennas operating in the 2.4 GHz band, and shorter brown strips display the dipole antennas working in the 5.8 GHz band. In addition, the parallel grey strips represent the feeding network (CPS) that excites the four dipole antennas. The four dipole antennas, together with the CPS, lie on the same layer of a Rogers 4350 B substrate with a relative permittivity of 3.66 and a loss tangent of 0.037. The longer and shorter dipole antennas are fed via the CPS to constitute dual-band W8JK arrays, achieving directional radiation patterns in both 2.4 and 5 GHz bands. Note that the sequence of the four dipoles in Figure 2 has been studied, and the proposed arrangement might be the most suitable choice to achieve dual-band directional radiation characteristics.

For the geometry of a dipole on a semi-infinite substrate, the formulation for the effective length of the dipole antenna was proposed in [3] using the moment method in the Fourier transform domain, which reads

$$L = 0.48\lambda_0 \frac{1}{(1 + W/L)\sqrt{1 + \varepsilon_1/2}}, \quad (1)$$

where is the free-space wavelength, W denotes the width of the dipole antenna, L represents the total length of the dipole antenna, and is the relative permittivity of the substrate. (1) can be utilized to ensure the effective lengths of the dipole antennas. Since (1) is based on the assumption that the substrate is infinite [3], three-dimensional full-wave electromagnetic simulation software is further applied to optimize the dipole lengths. The underlying theory and design principles will be discussed below.

First, to provide an insight into the dual-band operating mechanism, the simulated reflection coefficients and the input impedances of three different cases (case 1: without longer dipole antennas; case 2: without shorter dipole antennas; case 3: the proposed antenna) are presented for comparison in Figures 3 and 4. The antenna in case 1 can only resonate at 5.8 GHz while the antenna in case 2 operates

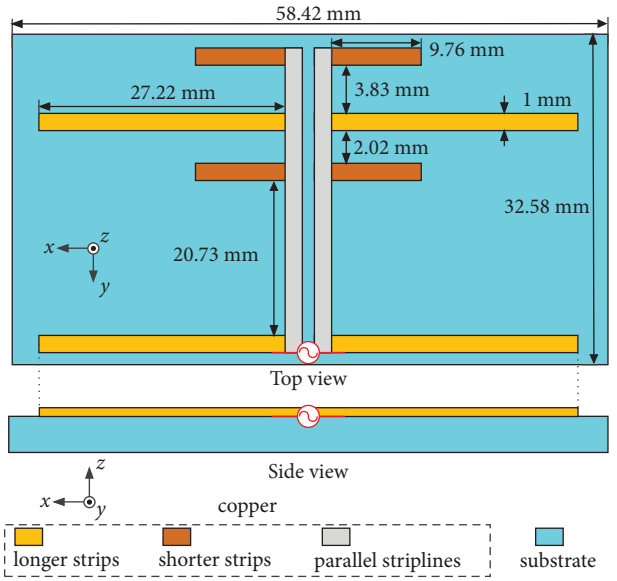


Figure 2: Configuration of the proposed dual-band directional radiation antenna.

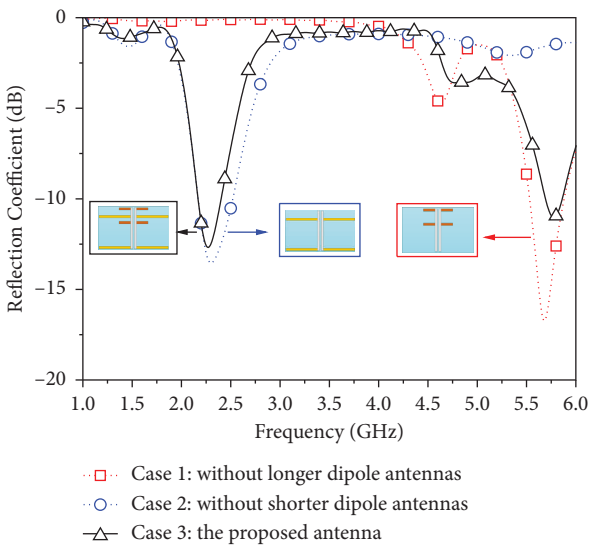


Figure 3: Simulated reflection coefficients of different cases (case 1: without longer strips; case 2: without shorter strips; and case 3: proposed antenna).

in the 2.4 GHz band, which is depicted in Figure 3. The comparison reveals that the resonances in 2.4 and 5.8 GHz bands are driven by longer and shorter dipole antennas, respectively, which can guide the design process to adjust the resonance frequencies separately. Moreover, as illustrated in Figure 4, the simulated input impedances of the antennas in different cases can better demonstrate the resonance mechanism for dual-band characteristics. The comparison between the input impedances in cases 1 (without a longer dipole antenna) and 3 (the proposed antenna) shows that the imaginary part in case 1 gets roughly 200 Ω at 2.4 GHz, as illustrated in Figure 4. Hence, the structure with only shorter dipole antennas can hardly achieve good input impedance matching at 2.4 GHz. Similarly, the imaginary part curve in

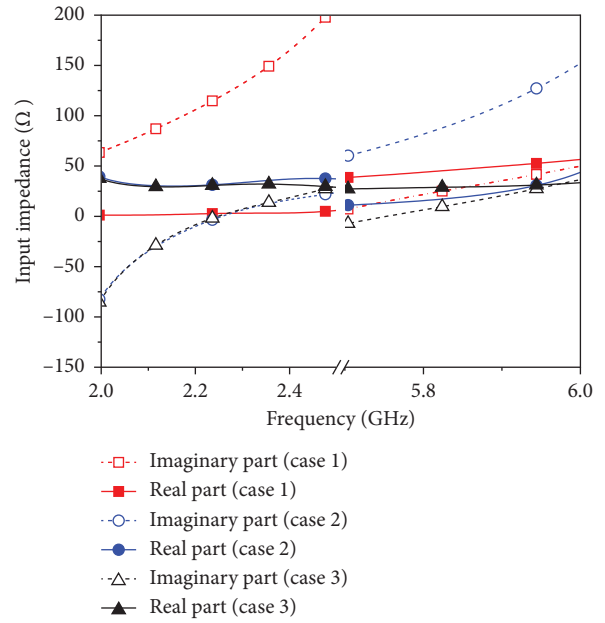


Figure 4: Simulated input impedances (real and imaginary parts) of different cases (case1: without longer strips; case 2: without shorter strips; and case 3: proposed antenna).

case 2 (without shorter dipole antennas) goes up to a high value with its real part approaching to 0 Ω at 5.8 GHz, indicating that the structure with only longer dipole antennas cannot achieve good resonance in the 5.8 GHz band. In conclusion, the fact that the resonances for the lower and the higher frequencies are driven by the longer and shorter dipole antennas, separately, is illustrated in Figures 3 and 4.

Second, the vector surface current distributions at both 2.4 and 5.8 GHz are studied by the simulation to show the mutual coupling effects, as illustrated in Figure 5. At 2.4 GHz, most of the surface currents concentrate on the longer dipoles. Moreover, the surface current distribution on the shorter dipoles seems stronger than that on the longer dipoles at 5.8 GHz. As a result, the longer and shorter dipole antennas can achieve good impedance matching at different frequencies without much mutual effect to decrease the radiation performance.

Third, the directional behaviour of the proposed antenna has also been studied according to vector surface current distributions shown in Figure 5. Note that the dipole antenna array theory can be utilized to better clarify the working principle of the directional behaviour. As depicted in Figure 5(a), the current distribution on the longer dipole antennas plays a decisive role in the directional radiation performance at the lower frequency (2.4 GHz). Moreover, the red lines with arrows, which indicate the direction of the vector surface current on the two longer dipole antennas, are opposite in direction. The antiphase of the surface current distribution on the two longer dipole antennas has thus been observed. Furthermore, the blue point on the CPS depicted in Figure 5(a) also indicates that the phase shift occurs as the vector surface current travels along the CPS. The longer dipole antenna away from the feeding port has a lagging phase compared with that close to the feeding port. According to the theoretical analysis in [12], the directional behaviour can be explained by the mechanism of the W8JK array, and the main

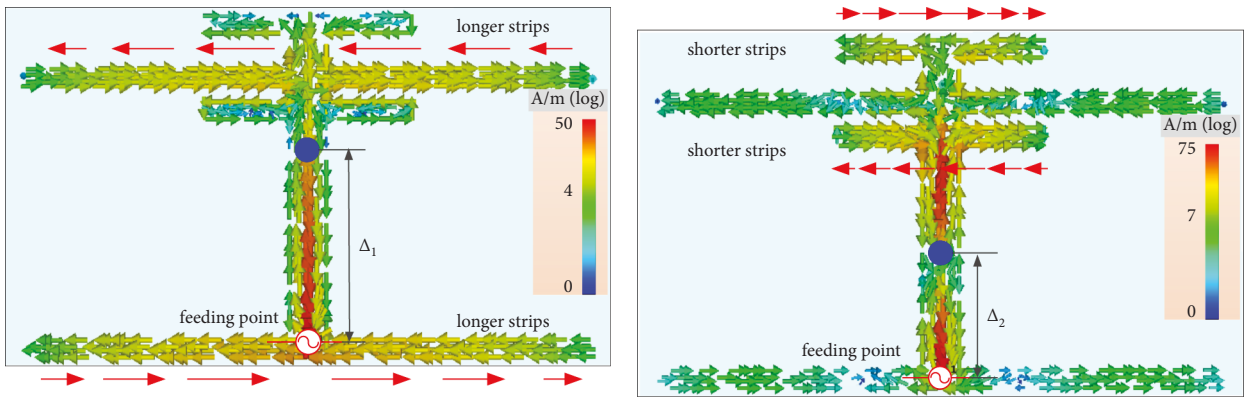


(a) (b)

Figure 5: Current distribution of the proposed antenna at 2.4/5.8 GHz (a) at 2.4 GHz (b) at 2.4 GHz.

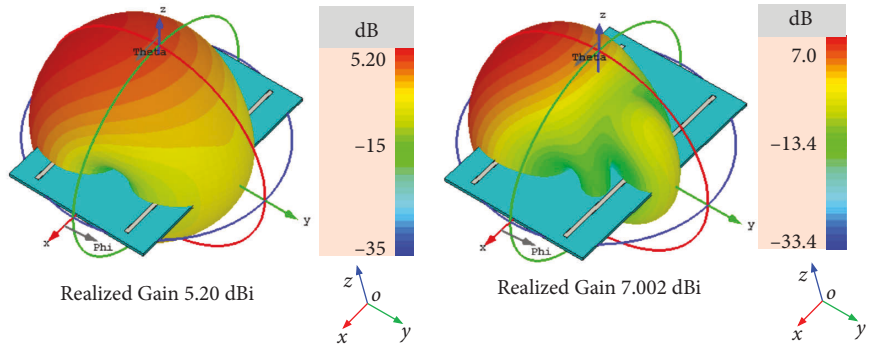


(a) (b)

Figure 6: Simulated radiation patterns: (a) at 2.4 GHz and (b) at 5.8 GHz.

beam would point to the dipole antenna with a lagging phase. At the higher frequency (5.8 GHz), an antiphase excitation can also be obtained by the feeding network (CPS), as shown in Figure 5(b), which shares the same mechanism with that at the lower frequency (2.4 GHz).

To further investigate the positions of the phase shift points shown in Figures 5(a) and 5(b), the effective permittivity ($\varepsilon_{\text{eff}}$) of the CPS should be calculated according to the electric and magnetic field distributions [9, 13]. Then, the phase shift positions can be approximated by following the equation:$\Delta_i = \lambda_0/4\sqrt{\varepsilon_{eff}}$, (2) where $\varepsilon_{\text{eff}} i = 1$, (2) refers to the distance between the phase shift points and the feeding points shown in Figures 5(a) and 5(b), $\lambda_0$ is the wavelength in free-space, and refers to the effective permittivity. Also, $\varepsilon_{\text{eff}}$ can be calculated by the following equations:

$$\sqrt{\varepsilon_{eff}(f)} = \sqrt{\varepsilon_q} + \frac{\left(\sqrt{\varepsilon_r} - \sqrt{\varepsilon_q}\right)}{\left(1 + a\left(f/f_{\text{te}}\right)^{-b}\right)},$$

$$f_{te} = \frac{c}{4d\sqrt{1-\varepsilon_r}}, \tag{3}$$

$$\varepsilon_q = \frac{1+\varepsilon_1}{2},$$

where $f_{\text{te}}$ is the cut-off frequency for the lowest order TE mode, $\varepsilon_q$ refers to the effective permittivity at the quasi-static limit, $d$ is the thickness of the substrate, and $a$ and $b$ are constants, which depend on the configuration and dimension of the CPS. For the configuration of the CPS proposed in this letter, the parameters $a$ and $b$ are approximately 1.8 and 4.0, respectively [9, 13].

To validate the directional radiation, the simulated 3D radiation patterns at 2.4 GHz and 5.8 GHz are presented in Figure 6. The directional radiation performance is obtained with the simulated gains of 5.2 dBi at 2.4 GHz and 7.0 dBi at 5.8 GHz, respectively. Also, ahigh front-to-back (F/B) ratio (up to 15 dB) is achieved in both the 2.4 GHz and 5.8 GHz bands, which is promising for directional antenna applications, and the F/B ratio among the whole operating bands is illustrated in Figure 7. Also, the realized gain and the efficiency over the frequency are illustrated in figures 8 and 9. Realized gains higher than 5 dBi/6 dBi can be observed among the lower and the higher bands of the proposed antenna. Moreover, the efficiency of the proposed antenna is up to 90% both for simulated and measured results, indicating the proposed antenna achieves a reasonable radiation characteristic.

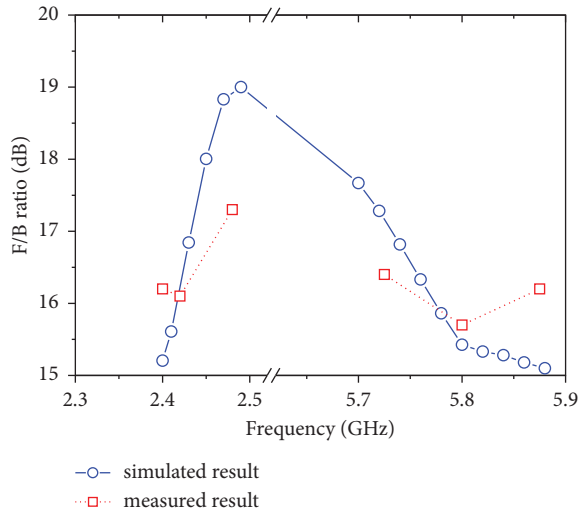


Figure 7: Simulated and the measured F/B ratio over the operating bands of the proposed directional antenna.

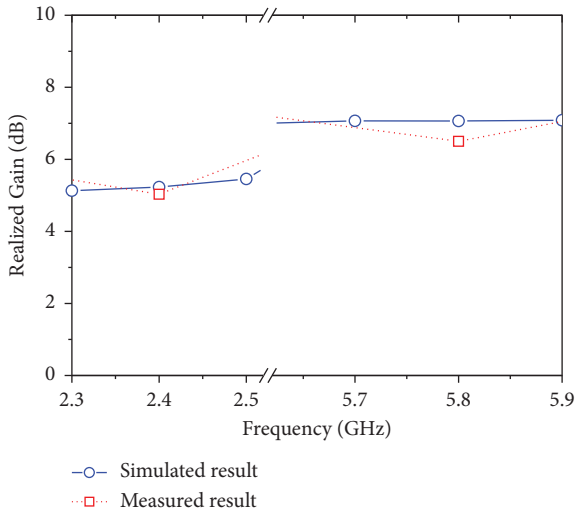


Figure 8: Simulated and the measured realized gain over the operating bands of the proposed directional antenna.

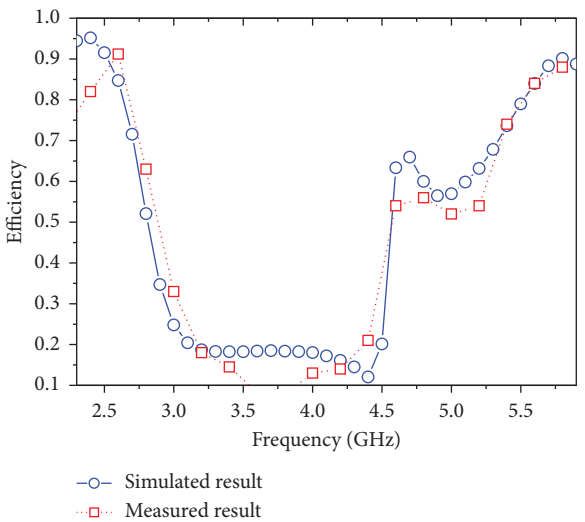


Figure 9: Simulated and the measured efficiency over the operating bands of the proposed directional antenna.

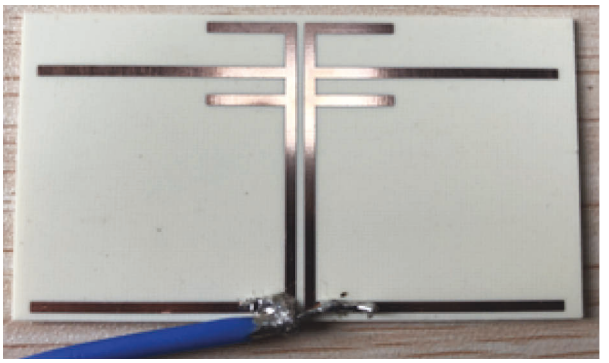

Figure 10: The fabricated prototype of the proposed antenna.

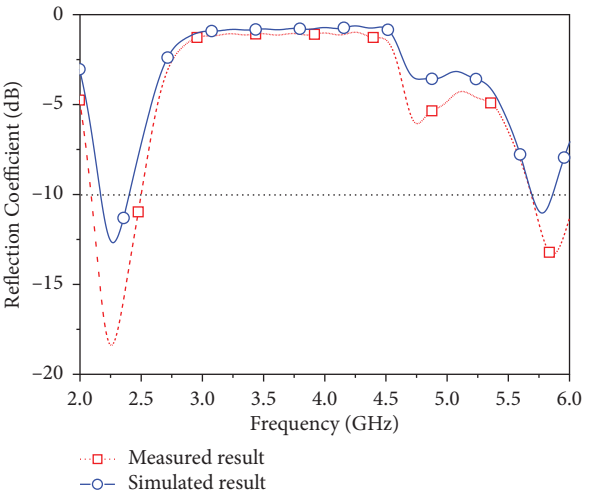


Figure 11: Measured and simulated reflection coefficient of the proposed antenna.

## 3. Results and Discussion

A prototype of the proposed antenna is fabricated, as depicted in Figure 10. It can be seen that the proposed antenna is on the top layer of a Rogers 4350 B substrate with a thinness of

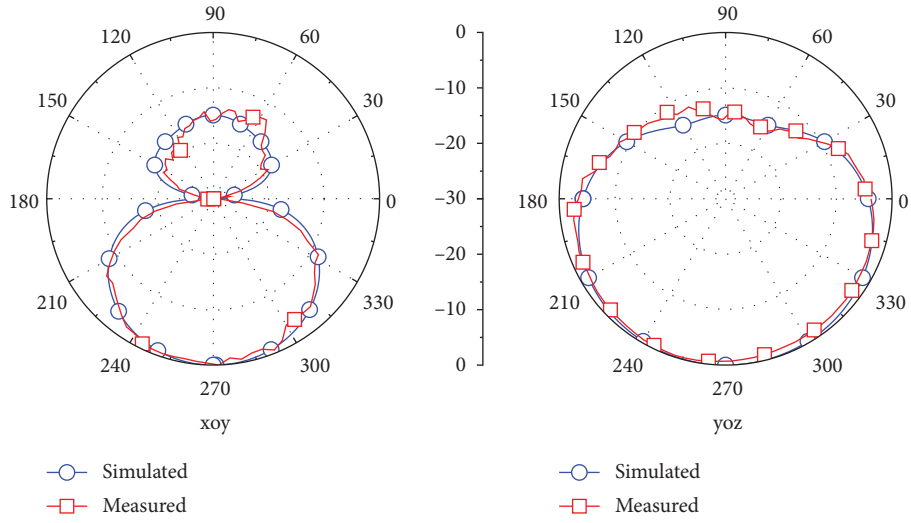


Figure 12: Simulated and measured radiation patterns at 2.4 GHz.

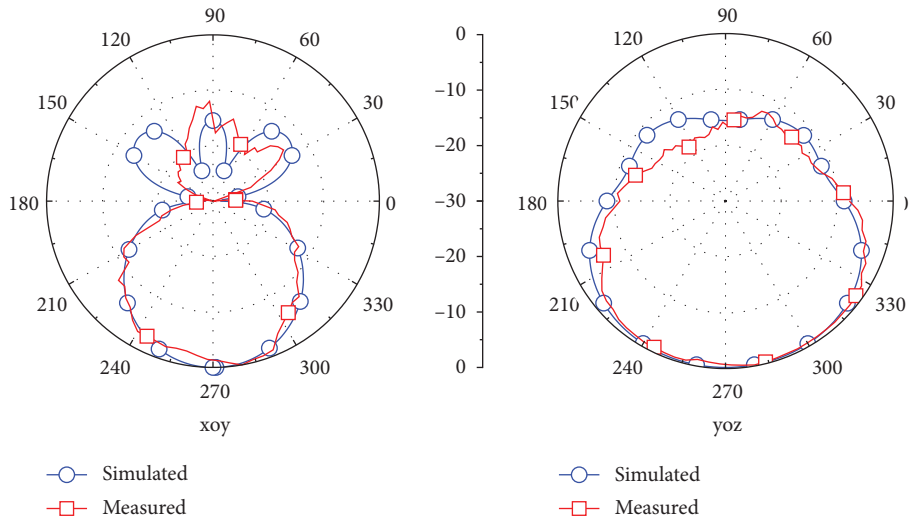


Figure 13: Simulated and measured radiation patterns at 5.8 GHz.

0.762 mm. A 50 Ω-coaxial cable is utilized to feed the proposed antenna through the CPS. The measured and simulated reflection coefficients of the proposed antenna are presented in Figure 11. Good agreement can be observed. The minor disagreement may be caused by the asymmetry of the feeding point and the existence of the coaxial line. The measurements were carried out with a Keysight vector network analyzer N5224A. In addition, the 2-D radiation patterns of the *xoz*-plane and *yoz*-plane were also measured in a SATIMO chamber, as shown in Figures 12 and 13. The measured gain is 5.4 and 7 dBi, respectively, in the 2.4 and 5.8 GHz bands. Note that the measured *F*/*B* ratio is presented in Figure 7, which is up to 15 dB over the dual-operating bands.

## 4. Conclusions

A low-profile dual-band directional antenna is proposed in this letter. The antenna successfully demonstrates how to realize a dual-band directional radiation characteristic utilizing four dipole antennas. Moreover, the dipole antennas with different lengths can work separately without much mutual effect, which simplifies the complexity of the design process. The directional radiation patterns have been achieved at 2.4 and 5.8 GHz without any metallic reflectors. The extremely low profile makes it possible to integrate the proposed antenna into the UAV's remote-control unit. A simplified CPS acting as a feeding network is utilized in the letter to achieve the W8JK array excitation requirement. Finally, the measured and simulated results verify that the proposed low-profile dual-band directional antenna would be a promising candidate for UAV applications with a high F/B ratio of up to 15 dB.

## Data Availability

All data, models, and code generated or used during the study appear in the submitted article.

## Conflicts of Interest

The authors declare that they have no conflicts of interest.

## Acknowledgments

This work was supported by the Natural Science Foundation of Fujian Province (2021J05178), Scientific Research Foundation of Jimei University (ZQ2021001) and Natural Science Foundation of China (12104027).

## References

[1] G. Virone, A. M. Lingua, M. Piras et al., "Antenna pattern verification system based on a micro unmanned aerial vehicle (UAV)," *IEEE Antennas and Wireless Propagation Letters*, vol. 13, pp. 169–172, 2014.

[2] E. E. Altshuler, T. H. O'Donnell, A. D. Yaghjian, and S. R. Best, "A monopole superdirective array," *IEEE Transactions on Antennas and Propagation*, vol. 53, no. 8, pp. 2653–2661, Aug, 2005.

[3] M. Alibakhshikenari, B. S. Virdee, C. H. See et al., "Dual-polarized highly folded bowtie antenna with slotted self-grounded structure for sub-6 GHz 5G applications," *IEEE Transactions on Antennas and Propagation*, vol. 70, no. 4, pp. 3028–3033, April 2022.

[4] S. R. Best, E. E. Altshuler, A. D. Yaghjian, J. M. McGinthy, and T. H. O'Donnell, "An impedance-matched 2-element superdirective array," *IEEE Antennas and Wireless Propagation Letters*, vol. 7, pp. 302–305, 2008.

[5] J. D. Kraus and R. J. Marhefka, *Antennas For All Applications, 3rded*, McGraw-Hill, New York, NY, USA, 2002.

[6] M. van Rooyen, J. W. Odendaal, and J. Joubert, "High-gain directional antenna for WLAN and WiMAX applications," *IEEE Antennas and Wireless Propagation Letters*, vol. 16, pp. 286–289, 2017.

[7] Z. Wang, G. x. Zhang, Y. Yin, and J. Wu, "Design of a dual-band high-gain antenna array for WLAN and WiMAX base station," *IEEE Antennas and Wireless Propagation Letters*, vol. 13, pp. 1721–1724, 2014.

[8] X. Quan, R. Li, G. Jin, and M. M. Tentzeris, "Development of a directional dual-band planar antenna for wireless applications," *IET Microwaves, Antennas & Propagation*, vol. 7, no. 4, pp. 245–250, 19 March 2013.

[9] R. Garg, I. Bahl, and M. Bozzi, *Microstrip Lines and Slotlines*, Artech House, Norwood, MA, USA, 2013.

[10] Y. Xiao, Y. Qi, F. Li, J. Fan, W. Yu, and L. Lu, "Dual-band directional slot antenna for Wi-Fi application," *IEEE Transactions on Antennas and Propagation*, vol. 66, no. 8, pp. 4277–4281, Aug, 2018.

[11] X. Quan, R. Li, Y. Cui, and M. M. Tentzeris, "Analysis and design of a compact dual-band directional antenna," *IEEE Antennas and Wireless Propagation Letters*, vol. 11, pp. 547–550, 2012.

[12] J. Wu, Z. Zhao, Z. Nie, and Q. H. Liu, "Design of anti-phase feeding network for W8JK array based on in-phase power divider," *IEEE Transactions on Antennas and Propagation*, vol. 62, no. 5, pp. 2870–2873, May 2014.

[13] M. Y. Frankel, S. Gupta, J. A. Valdmanis, and G. A. Mourou, "Terahertz attenuation and dispersion characteristics of co-planar transmission lines," *IEEE Transactions on Microwave Theory and Techniques*, vol. 39, no. 6, pp. 910–916, June 1991.

[14] R. Wu and Q. Chu, "Multi-mode broadband antenna for 2G/3G/LTE/5G wireless communication," *Electronics Letters*, vol. 54, no. 10, pp. 614–616, May 2018.

[15] A. Papathanasopoulos and Y. Rahmat-Samii, "Transmitarray antenna for conical beam scanning," *IEEE Trans. Antennas Propag., early access*, 2022.

[16] M. Alibakhshikenari, B. S. Virdee, P. Shukla et al., "Impedance bandwidth improvement of a planar antenna based on metamaterial-inspired T-matching network," *IEEE Access*, vol. 9, pp. 67916–67927, 2021.

[17] M. Mirmozafari, R. Ma, F. T. Dagefu, and N. Behdad, "A compact wideband multi-beam antenna for VHF/UHF directional networking applications," *IEEE Trans. Antennas Propag., early access*, 2022.

[18] M. Kominami, D. Pozar, and D. Schaubert, "Dipole and slot elements and arrays on semi-infinite substrates," *IEEE Transactions on Antennas and Propagation*, vol. 33, no. 6, pp. 600–607, June 1985.